REGULAR ARTICLE

blood advances

EVI1 exerts distinct roles in AML via ERG and cyclin D1 promoting a chemoresistant and immune-suppressive environment

Yosuke Masamoto,[1] Akira Chiba,[1] Hideaki Mizuno,[1] Toshiya Hino,[1] Hiroki Hayashida,[1] Tomohiko Sato,[1,2] Masashige Bando,[3] Katsuhiko Shirahige,[3] and Mineo Kurokawa[1,4]

[1]Department of Hematology & Oncology, Graduate School of Medicine, The University of Tokyo, Tokyo, Japan; [2]Division of Transfusion Medicine and Cell Therapy, The Jikei University Hospital, Tokyo, Japan; [3]Laboratory of Genome Structure and Function, Research Center for Epigenetic Disease, Institute for Molecular and Cellular Biosciences, The University of Tokyo, Tokyo, Japan; and [4]Department of Cell Therapy and Transplantation, The University of Tokyo Hospital, Tokyo, Japan

Key Points

- EVI1 exerts distinct roles in AML, including resistance, pathogenicity of aggressive diseases independent of stemness, and immune evasion.
- ERG and cyclin D1 are leukemia-specific targets of EVI1, providing potential therapeutic vulnerability of EVI1-associated AML.

Aberrant expression of ecotropic viral integration site-1 (*EVI1*$^{+}$) is associated with very poor outcomes in acute myeloid leukemia (AML), mechanisms of which are only partially understood. Using the green fluorescent protein reporter system to monitor *EVI1* promoter activity, we demonstrated that *Evi1*^{high} KMT2A-MLLT1–transformed AML cells possess distinct features from *Evi1*^{low} cells: the potential for aggressive disease independent of stem cell activity and resistance to cytotoxic chemotherapy, along with the consistent gene expression profiles. RNA sequencing and chromatin immunoprecipitation sequencing in EVI1-transformed AML cells and normal hematopoietic cells combined with functional screening by cell proliferation–related short hairpin RNAs revealed that the erythroblast transformation–specific transcription factor ERG (E26 transformation-specific [ETS]-related gene) and cyclin D1 were downstream targets and therapeutic vulnerabilities of *EVI1*$^{+}$ AML. Silencing *Erg* in murine *EVI1*$^{+}$ AML models severely impaired cell proliferation, chemoresistance, and leukemogenic capacity. Cyclin D1 is also requisite for efficient EVI1-AML development, associated with gene expression profiles related to chemokine production and interferon signature, and T- and natural killer–cell exhaustion phenotype, depending on the interferon gamma (IFN-γ)/STAT1 pathway but not on CDK4/CDK6. Inhibiting the IFN-γ/STAT1 pathway alleviated immune exhaustion and impaired EVI1-AML development. Overexpression of EVI1 and cyclin D1 was associated with IFN-γ signature and increased expression of chemokines, with increased exhaustion molecules in T cells also in human AML data sets. These data collectively suggest that ERG and cyclin D1 play pivotal roles in the biology of *EVI1*$^{+}$ AML, where ERG contributes to aggressive disease nature and chemoresistance, and cyclin D1 leads to IFN-γ signature and exhausted T-cell phenotypes, which could potentially be targeted.

Introduction

Acute myeloid leukemia (AML) represents a heterogeneous group of neoplasms.[1] Although molecular-targeted therapy has been realized for some disease types with targetable gene mutations,[2-4] many refractory subtypes of AML still remain.

Submitted 4 May 2022; accepted 22 September 2022; prepublished online on *Blood Advances* First Edition 21 October 2022; final version published online 14 April 2023. https://doi.org/10.1182/bloodadvances.2022008018.

Anti-FLAG ChIP-seq and RNA-seq data are available through Sequence Read Archive (accession numbers PRJNA615776 and DRA014515).

Data are available on request from the corresponding author, Mineo Kurokawa (kurokawa@m.u-tokyo.ac.jp).

The full-text version of this article contains a data supplement.

Ecotropic viral integration site-1 (*EVI1*) is encoded by the MDS1 and EVI1 complex locus (MECOM).[5] In mice, aberrant expression of EVI1 causes myelodysplasia-like conditions or AML.[6-8] Increased expression of EVI1, found in approximately 8% of de novo AML, has been related to very poor clinical outcomes.[9,10] In *EVI1*^{high} (*EVI1*$^{+}$) AML, inv(3)(q21q26) or t(3;3)(q21;q26) are recurrently identified, both of which result in translocation of a distal enhancer of *GATA2* gene to *MECOM*,[11,12] leading to overexpression of *EVI1* and decreased *GATA2* expression.[13,14] Other mechanisms of *EVI1* overexpression in AML include atypical translocation of 3q26 and translocations affecting *KMT2A* on 11q23, whereas not all mechanisms have been clarified.[15] Despite the need for specific targeting measures against *EVI1*$^{+}$ AML, they have not yet been achieved, mainly owing to a lack of knowledge about its downstream targets,[16,17] whereas some metabolic vulnerabilities have been reported.[18,19]

ERG (E26 transformation-specific [ETS]-related gene) is a member of the erythroblast transformation–specific (ETS) transcription factor family, implicated in the function of the hematopoietic stem cells (HSCs).[20,21] ERG has also been reported as an oncogene in multiple malignancies.[22-25] Despite numerous studies, the mechanisms by which ERG is upregulated in each subtype of AML, the molecular action by which ERG contributes to leukemogenesis, and the potential of ERG as a therapeutic target remains only partially understood.[26-28]

Cyclin D, a major oncogenic driver in many tumors, is an allosteric regulator of CDK4/CDK6 kinases, controlling cell cycle progression from G1 to S phase.[29,30] Recent studies have demonstrated various oncogenic functions of cyclin D1 besides cell cycle regulation, including transcriptional regulation.[31,32] Cyclin D1 and associated kinases have multifaceted functions, including antitumor immunity.[33-36] Despite rapidly expanding knowledge of cyclin D1 in cancer biology, the role of cyclin D1 in AML remains poorly understood.[37-40]

Recently, immune escape of AML cells has been receiving increasing attention.[41] Despite advances in anti-AML treatments, only a limited proportion can be cured without allogeneic HSC transplantation, underscoring the potential efficacy of immunotherapies. However, complex mechanisms of AML immune escape have hampered the development of immunotherapies. In addition to cell-intrinsic factors, the importance of altered immunologic milieu has been reported,[42] as shown mainly in solid tumors.[43,44] Interferon gamma (IFN-γ)-related gene expression profiles have recently been associated with resistance in AML,[45] which is of great interest because much attention has lately been paid to the role of IFN-γ in promoting immune exhaustion through the expression of inhibitory molecules that limits antitumor immunity,[46,47] although IFN-γ was initially thought to be an antitumor cytokine.[48,49] However, the mechanisms by which the tumor microenvironment leads to the refractoriness of AML and the role of IFN-γ in shaping this microenvironment are still unclear.

In this study, we comprehensively investigated the potential downstream targets of EVI1 and examined the role of ERG and cyclin D1 in an *EVI1*$^{+}$ AML model as possible candidate genes.

Methods

Mice

All experiments were approved by The University of Tokyo Ethics Committee for Animal Experiments and strictly adhered to the guidelines for animal experiments.

Retrovirus production, transduction, and cell selection

The production of retroviruses and transduction was performed as previously described with a slight modification.[8]

Flow cytometry

The list of antibodies used is provided in supplemental Table 1. Stained samples were sorted with FACS Aria II, Aria III, or analyzed with FACSCelesta (BD).

Chromatin immunoprecipitation sequencing (ChIP-seq) analysis

ChIP experiments were carried out as previously described.[8] The list of primers used in quantitative polymerase chain reaction (qPCR) is provided in supplemental Table 2. Sequencing libraries were prepared using NEBNext Ultra II DNA library kit for Illumina (NEB) according to the instruction manual, and sequenced, single-end 65-bp reads, on the Illumina HiSeq2500 system. The data were analyzed as previously described.[19]

RNA sequencing (RNA-seq) analysis

RNA-seq for green fluorescent protein–high (GFP^{high}) and –low (GFP^{low}) cells from KMT2A-MLLT1 AML mice were performed using freshly isolated 2 × 10^5 leukemic granulocyte-monocyte progenitor (L-GMP) cells (n = 2 for GFP^{high} and GFP^{low}, each). The top 5% and bottom 5% of cells were collected based on GFP intensity. To obtain each sample, 2 different AML mice were used.

RNA-seq for sh*Erg* and sh*Ccnd1* was performed using 2 × 10^6 puromycin-selected EVI1-AML cells (n = 2). RNA-seq for sh*Ccnd1* was performed using freshly isolated 2 × 10^6 EVI1-AML GFP^{+} c-kit^{+} bone marrow (BM) cells (n = 5-6). TPMCalculator was used to calculate the transcript per million value of a gene in each sample with the default parameters.[50]

Data analysis using publicly available genetic data

The genetic data of The Cancer Genome Atlas and Oregon Health & Science University cohorts[51,52] were obtained via cBioPortal.[53,54]

CIBERSORTx analysis

CIBERSORTx analysis was performed according to the authors' instructions.[55] Signature matrix files publicly provided by the authors were used.

Statistical analysis

Statistical significance of differences was assessed using a two-tailed unpaired Student *t* test. For the survival analysis, a log-rank test was used on the R software (version 4.0.5).

Results

Evi1^{high} cells show distinct features in murine AML models

To investigate the expression pattern of *EVI1* in AML, we used human AML single-cell RNA-seq data.[56] In patients with *EVI1*$^{+}$ AML with inv(3)(q21.3q26.2) and t(9;11)(p21;q23), *EVI1* expression in AML cells was heterogeneous (Figure 1A-B and supplemental Figure 1A-B). We generated an AML mice model using lineage^{-} Sca-1^{+} c-kit^{+} (LSK) cells from *Evi1-GFP* KI mice, in which the *Evi1-IRES-GFP* allele was inserted into the *MECOM* locus to allow monitoring of *Evi1* expression by GFP intensity.[57] Oncogenic fusion gene *KMT2A-MLLT1,* known to upregulate *Evi1*,[58] was transduced into KI LSK cells with *Kusabira-Orange* (*KuO*) and transplanted into syngeneic mice (Figure 1C). Each AML mouse showed heterogeneous positivity of GFP, whereas GFP^{high} cells were not enriched in L-GMPs with high leukemia stem cell activity (Figure 1D and supplemental Figure 1C). GFP^{high} L-GMPs demonstrated higher expression of *Evi1* than GFP^{low} L-GMPs with comparable KuO levels (Figure 1E and supplemental Figure 1D).

Because *Evi1*^{high} cells were associated with high stem cell activity in normal hematopoiesis,[57] we investigated the hierarchical structure of KMT2A-MLLT1 AML. Both GFP^{high} and GFP^{low} cells can generate both GFP^{high} and GFP^{low} L-GMPs in secondary recipients (supplemental Figure 1E). The colony-forming activity of GFP^{high} L-GMPs differed between individual mice, whereas GFP^{low} L-GMPs showed consistently high activity (Figure 1F). Similarly, when GFP^{high} and GFP^{low} L-GMPs were transplanted into recipient mice, the leukemogenic potential of GFP^{high} L-GMPs was variable. When GFP^{high} L-GMPs reconstituted AML, the recipient mice succumbed more rapidly than those engrafted with GFP^{low} L-GMPs (Figure 1G-H and supplemental Figure 1F). These results are independent of low stem cell activity, indicated by the low frequency of mice showing AML engraftment followed by the development of fatal AML after infusion of GFP^{high} L-GMPs (Figure 1I and supplemental Figure 1G-H). When we administered cytarabine to mice with KMT2A-MLLT1 AML harboring the *Evi1*-KI allele, GFP^{high} cells were enriched in the BM live cells of cytarabine-treated mice (Figure 1J).

When we performed RNA-seq of freshly isolated GFP^{high} and GFP^{low} L-GMPs within the same KMT2A-MLLT1 primary AML mice to characterize GFP^{high} cells, gene set enrichment analysis showed enrichment of several pathways (Figure 1K-L). Intriguingly, GFP^{high} L-GMPs showed an opposite expression pattern to leukemic stem cells (Figure 1M and supplemental Figure 1I). Gene sets associated with resistance to chemotherapeutic drugs are upregulated in GFP^{high} L-GMPs (Figure 1N and supplemental Figure 1J). Consistently, additive retroviral overexpression of EVI1 in established KMT2A-MLLT1 AML cells led to decreased colony-forming and leukemogenic capacity (Figure 1O and supplemental Figure 1K-L). These findings suggest that *EVI1*^{high} L-GMPs are associated with aggressive disease features and chemoresistance rather than stem cell activity.

EVI1 binds to promoter regions of *ERG* and *CCND1* in AML cells

To identify the target genes of EVI1 in AML, we performed ChIP-seq analysis using EVI1-transformed AML (EVI1-AML) cells generated by transduction of 3× FLAG-tagged EVI1 into murine HSCs and progenitor cells followed by transplant.[8] In this model, AML develops after a long period of myelodysplastic syndrome or myeloproliferative neoplasm-like disease. EVI1-AML cells demonstrated approximately 8 times *Evi1* mRNA compared with normal LSKs (supplemental Figure 2A). After confirming the enrichment of previously reported EVI1-binding regions in the anti-FLAG ChIP samples (supplemental Figure 2B), these samples were applied to sequencing.[19] EVI1-binding regions tended to cluster around gene promoters (supplemental Figure 2C). To identify AML-specific regions, the results were compared with a murine myeloid progenitor cell line 32D-cl3, where a 3× FLAG-tag was inserted at the 3′-end of the *Evi1* locus (A.C., Y.M., H.M., M.B., K.S., and M.K., unpublished data, October 2022). They shared a relatively small number of binding regions (Figure 2A). Database for annotation, visualization and integrated discovery analysis revealed that AML-specific regions were enriched in genes involved in immune-related processes (Figure 2B).

To further narrow the list, we utilized RNA-seq data obtained from BM cells transduced with *EVI1*[19] (Figure 2C) and human transcriptome data.[9] We chose the common genes as candidates: binding of EVI1, upregulation by EVI1 transduction, and positive correlation with *EVI1* in human AML (Figure 2D-E). Short hairpin RNAs (shRNAs) against these candidate genes were transduced into EVI1-AML cells, along with fluorescent protein DsRed. Genes of which shRNA resulted in a continuous decrease in the frequency of DsRed^{+} cells, were considered positive (Figure 2F). Silencing of *Erg* and *Ccnd1* decreased DsRed^{+} cell populations, leading us to focus on ERG and cyclin D1 (Figure 2G). Importantly, EVI1-GFP^{high} L-GMPs in the KMT2A-MLLT1 AML mice showed high expression of *Erg* and *Ccnd1*, suggesting the possibility that these factors act as mediators of EVI1 (Figure 2H).

The ChIP-seq analysis showed that FLAG-EVI1 bound to the regulatory regions of *Erg* and *Ccnd1*, confirmed by ChIP-qPCR (Figure 3A-B and supplemental Figure 2D). Among them, a known *cis*-regulatory region of *Erg,* 85 kb downstream from the transcription start site (ERG+85) and a putative *cis*-regulatory region 4 kb downstream from the *Ccnd1* transcription start site (both to which multiple major HSC-regulating transcription factors bind), were activated by EVI1 in a luciferase reporter assay, whereas the EVI1 binding motif was not required for the activation (supplemental Figure 3A-F).[59-61] The corresponding regions in humans are DNase I sensitive in primary human AML cells with inv(3) and are bound by EVI1 in HNT-34, a human EVI1^{+} AML cell line (Figure 3C and supplemental Figure 3G-H). shRNAs against transduced *EVI1* decreased the expression of *Erg* and *Ccnd1*, suggesting the role of EVI1 in activating these genes (Figure 3D). Although the correlation between *MECOM* and *ERG* was not significant in the public expression data of human AML as a whole, there was a strong correlation in patients with 3q26 abnormalities (Figure 3E). The single-cell RNA-seq data from a patient with inv(3)(q21.3q26.2) AML demonstrated concordant expression between *MECOM* and *ERG* also at the cell level[56] (Figure 3F). GFP^{high} L-GMPs showed upregulation of ERG-fusion–associated as well as EWS/ETS-fusion–associated genes (supplemental Figure 3I-J). As for *CCND1*, the correlation with *MECOM* was confirmed in the whole cohort and patients with 3q26 rearrangement (Figure 3G-H).[51] Patients with *EVI1*$^{+}$ AML expressed a higher level of *CCND1* (Figure 3I). The decreased colony-forming activity

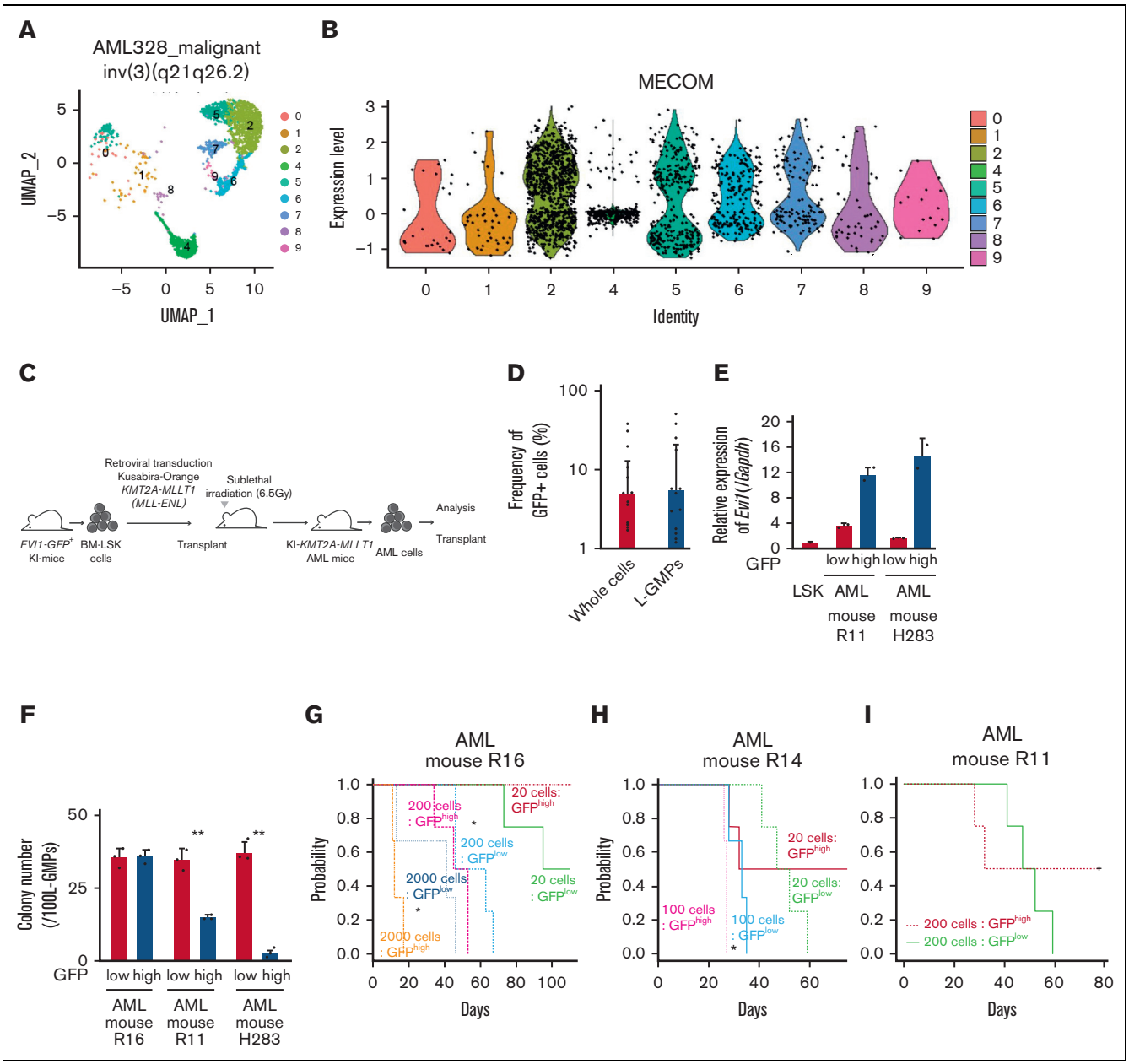

Figure 1. *Evi1*^{high} cells show distinct features in murine AML models. (A) Uniform manifold approximation and projection (UMAP) plot of single-cell RNA-seq (scRNA-seq) data of AML cells from patient AML328 with inv(3)(q21.3q26.2), showing 9 clusters. (B) Violin plot of MECOM expression in the 9 clusters. (C) The scheme of the experimental model of *EVI1-GFP KMT2A-MLLT1* AML mice. (D) Frequency of GFP$^+$ cells in the whole live KuO$^+$ AML cells and L-GMPs from the BM of *EVI1-GFP KMT2A-MLLT1* AML mice. (E) qPCR showing the relative expression of *Evi1* in GFP^{high} and GFP^{low} AML cells compared with normal LSKs. (F) Colony-forming units of GFP^{high} and GFP^{low} L-GMPs from 3 independent AML mice. (G-I) A Kaplan-Meier survival curve for secondary recipient mice that underwent transplantation with an indicated number of GFP^{high} or GFP^{low} L-GMPs, after exposure to 6.5 Gy total body irradiation (TBI). Significance between the same number of cells was examined by a log-rank test. (J) Frequency of GFP$^+$ cells in L-GMPs in secondary recipient mice intravenously treated with vehicle (phosphate-buffered saline) or cytarabine (AraC; 100 mg/kg) for 5 days through days 15 and 19 after transplant. Mice were analyzed on day 19. (K) Top-ranked differentially expressed genes between GFP^{high} and GFP^{low} L-GMPs. (L) Top-ranked pathways enriched in GFP^{high} L-GMPs. (M-N) Gene set enrichment analysis (GSEA) showing that downregulated genes in leukemia stem cells (M) and multiple drug-resistant–related genes (N) are upregulated in GFP^{high} L-GMPs. (O) Colony-forming units of 200 *KMT2A-MLLT1* AML cells with or without exogenous EVI1 expression from 3 independent primary recipients (supplemental Figure 1K). Mean ± standard deviation (SD). *$P < .05$, **$P < .01$, ***$P < .001$. FDR, false discovery rate (q value); NES, normalized enrichment score.

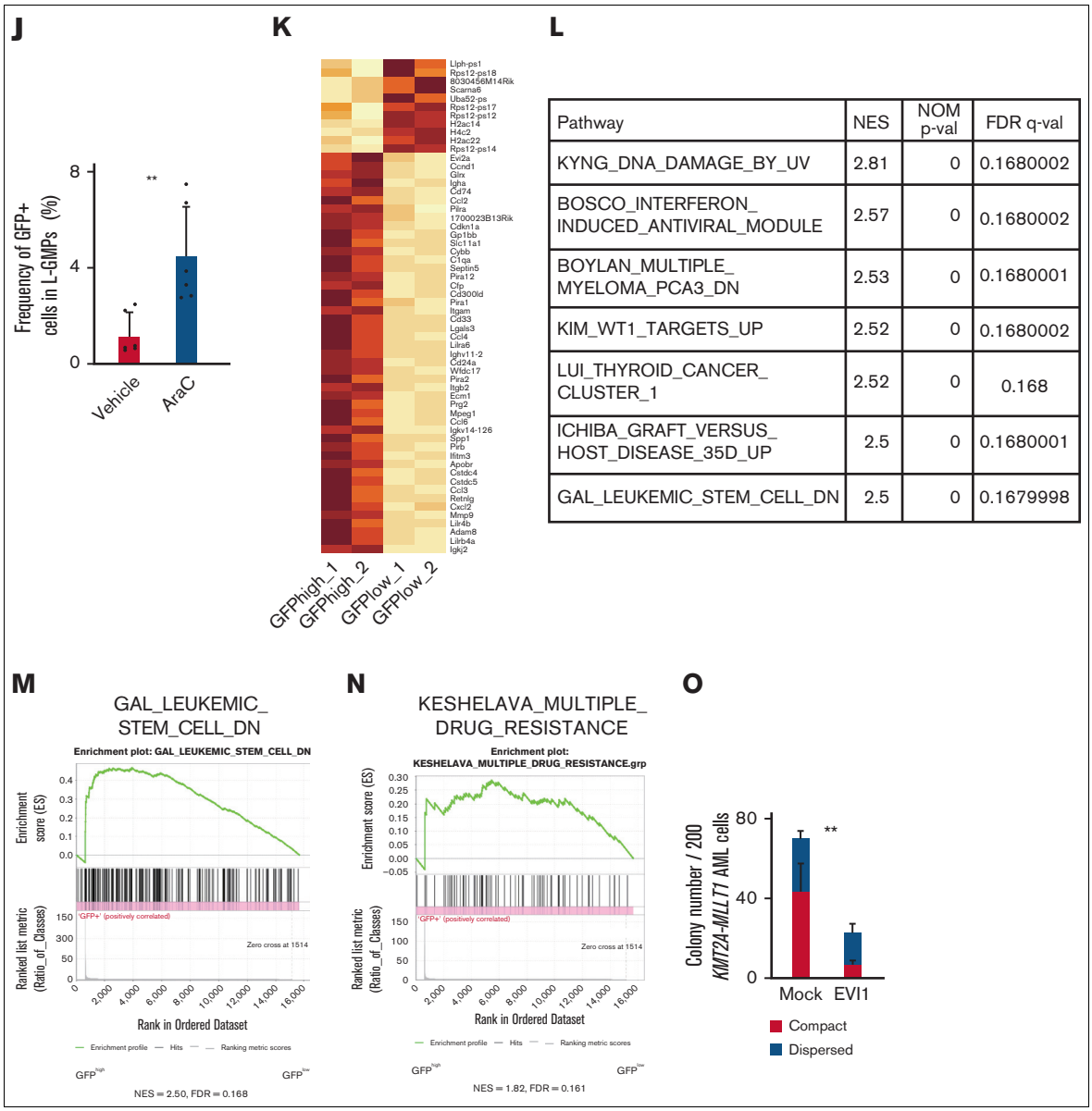

Pathway	NES	NOM p-val	FDR q-val
KYNG_DNA_DAMAGE_BY_UV	2.81	0	0.1680002
BOSCO_INTERFERON_ INDUCED_ANTIVIRAL_MODULE	2.57	0	0.1680002
BOYLAN_MULTIPLE_ MYELOMA_PCA3_DN	2.53	0	0.1680001
KIM_WT1_TARGETS_UP	2.52	0	0.1680002
LUI_THYROID_CANCER_ CLUSTER_1	2.52	0	0.168
ICHIBA_GRAFT_VERSUS_ HOST_DISEASE_35D_UP	2.5	0	0.1680001
GAL_LEUKEMIC_STEM_CELL_DN	2.5	0	0.1679998

Figure 1 (continued)

of *Evi1*-silenced c-kit^{+} normal hematopoietic progenitors did not seem to be mediated by *Erg* or *Ccnd1* (supplemental Figure 3K). These findings collectively indicate the promise of ERG and cyclin D1 as candidates for potential specific targets in EVI1-AML.

Evi1^{high} AML cells are dependent on ERG

The proliferation of EVI1-AML cells was susceptible to *Erg* silencing (Figure 4A and supplemental Figure 4A-B). EVI1-AML cells expressing sh*Erg* demonstrated diminished clonogenic activity (Figure 4B). Knockdown of *Erg* led to cell cycle arrest and apoptosis (supplemental Figure 4C-D). Silencing of *Erg* dramatically abrogated the leukemogenic potential of EVI1-AML cells in vivo (Figure 4C and supplemental Figure 4E).

To elucidate the functional relationship between EVI1 expression and dependency on ERG, we established immortalized cell lines by introducing KMT2A-MLLT1 into *Evi1-GFP* KI c-kit^{+} cells, followed by single-cell isolation (supplemental Figure 4F-G); an *Evi1*^{high} clone (CL2) with high GFP expression and dependency on EVI1, and an *Evi1*^{low} clone (CL1) without EVI1-dependency (Figure 4D and supplemental Figure 4H) was produced. The differential effect of *Erg* silencing was analyzed by using these lines. Knockdown of *Erg* in CL1 led to a marginal decrease in proliferation and no change in clonogenic ability (supplemental Figure 4I-J). In contrast, when *Erg* was silenced in CL2, substantial inhibition in cell growth and colony-forming activity was observed (Figure 4E-F). To assess the role of ERG in various AML models, we established MOZ-TIF2 and HOXA9-MEIS1 AML mice by retroviral transduction, both of which did not express *Evi1*.[62,63] Silencing of *Erg* did not affect the proliferation of MOZ-TIF2 and HOXA9-MEIS1 AML cells, like *Evi1*^{low} KMT2A-MLLT1-transformed cells (Figure 4G).

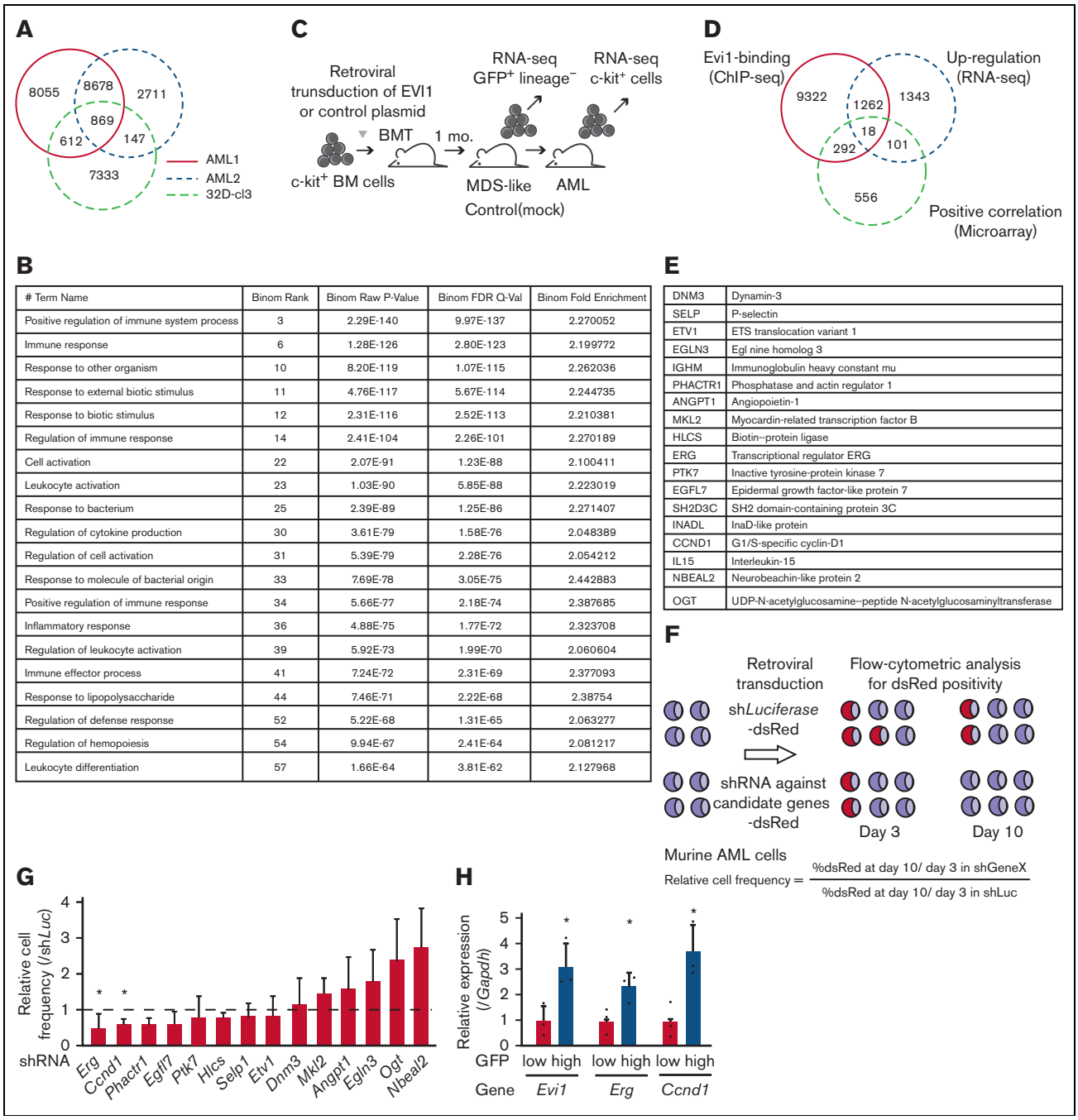

# Term Name	Binom Rank	Binom Raw P-Value	Binom FDR Q-Val	Binom Fold Enrichment
Positive regulation of immune system process	3	2.29E-140	9.97E-137	2.270052
Immune response	6	1.28E-126	2.80E-123	2.199772
Response to other organism	10	8.20E-119	1.07E-115	2.262036
Response to external biotic stimulus	11	4.76E-117	5.67E-114	2.244735
Response to biotic stimulus	12	2.31E-116	2.52E-113	2.210381
Regulation of immune response	14	2.41E-104	2.26E-101	2.270189
Cell activation	22	2.07E-91	1.23E-88	2.100411
Leukocyte activation	23	1.03E-90	5.85E-88	2.223019
Response to bacterium	25	2.39E-89	1.25E-86	2.271407
Regulation of cytokine production	30	3.61E-79	1.58E-76	2.048389
Regulation of cell activation	31	5.39E-79	2.28E-76	2.054212
Response to molecule of bacterial origin	33	7.69E-78	3.05E-75	2.442883
Positive regulation of immune response	34	5.66E-77	2.18E-74	2.387685
Inflammatory response	36	4.88E-75	1.77E-72	2.323708
Regulation of leukocyte activation	39	5.92E-73	1.99E-70	2.060604
Immune effector process	41	7.24E-72	2.31E-69	2.377093
Response to lipopolysaccharide	44	7.46E-71	2.22E-68	2.38754
Regulation of defense response	52	5.22E-68	1.31E-65	2.063277
Regulation of hemopoiesis	54	9.94E-67	2.41E-64	2.081217
Leukocyte differentiation	57	1.66E-64	3.81E-62	2.127968

DNM3	Dynamin-3
SELP	P-selectin
ETV1	ETS translocation variant 1
EGLN3	Egl nine homolog 3
IGHM	Immunoglobulin heavy constant mu
PHACTR1	Phosphatase and actin regulator 1
ANGPT1	Angiopoietin-1
MKL2	Myocardin-related transcription factor B
HLCS	Biotin--protein ligase
ERG	Transcriptional regulator ERG
PTK7	Inactive tyrosine-protein kinase 7
EGFL7	Epidermal growth factor-like protein 7
SH2D3C	SH2 domain-containing protein 3C
INADL	InaD-like protein
CCND1	G1/S-specific cyclin-D1
IL15	Interleukin-15
NBEAL2	Neurobeachin-like protein 2
OGT	UDP-N-acetylglucosamine--peptide N-acetylglucosaminyltransferase

Figure 2. A combination of multimodal screening showed potential targets of EVI1 in AML cells. (A) Venn diagram of ChIP-seq data using anti-FLAG antibody, showing FLAG-EVI1 binding regions. Two 3× FLAG-tagged EVI1-AML samples and a sample from 32D-cl3 murine hematopoietic progenitor cells where FLAG-tag was knocked in to the 3′-end of the *Mecom* locus. (B) Database for Annotation, Visualization and Integrated Discovery (DAVID) analysis showing AML-specific EVI1-binding regions. (C) A model of RNA-seq experiments. Genes upregulated at both early and late points after EVI1 introduction were chosen for further analysis. (D) Venn diagram of genes with EVI1-binding (ChIP-seq), upregulation after EVI1 transduction (RNA-seq), and positive correlation between EVI1 expression (microarray). (E) The list of genes in the common population of Figure 2D. (F) A scheme of the screening assay using DsRed. (G) Relative enrichment of DsRed^{+} cells expressing shRNA against each gene through days 3 and 10, adjusted by the sh*Luciferase* control. Significance was examined in comparison with the sh*Luciferase* control. (H) qPCR showing the relative expression of *Evi1*, *Erg*, and *Ccnd1* in GFP^{high} and GFP^{low} AML cells. Mean ± SD. *$P < .05$.

Knockdown of *Erg* significantly retarded *Evi1*-expressing KMT2A-MLLT1 AML development (Figure 4H). Corresponding to the persistence of *Evi1*^{high} cells after cytotoxic chemotherapy, we analyzed the effect of ERG on cell growth of EVI1-AML cells under daunomycin treatment in vitro. Although *Erg* knockdown significantly inhibited basal cell proliferation, it further enhanced sensitivity to daunomycin (Figure 4I). In contrast, the development of HOXA9-MEIS1 AML was not affected by *Erg* silencing

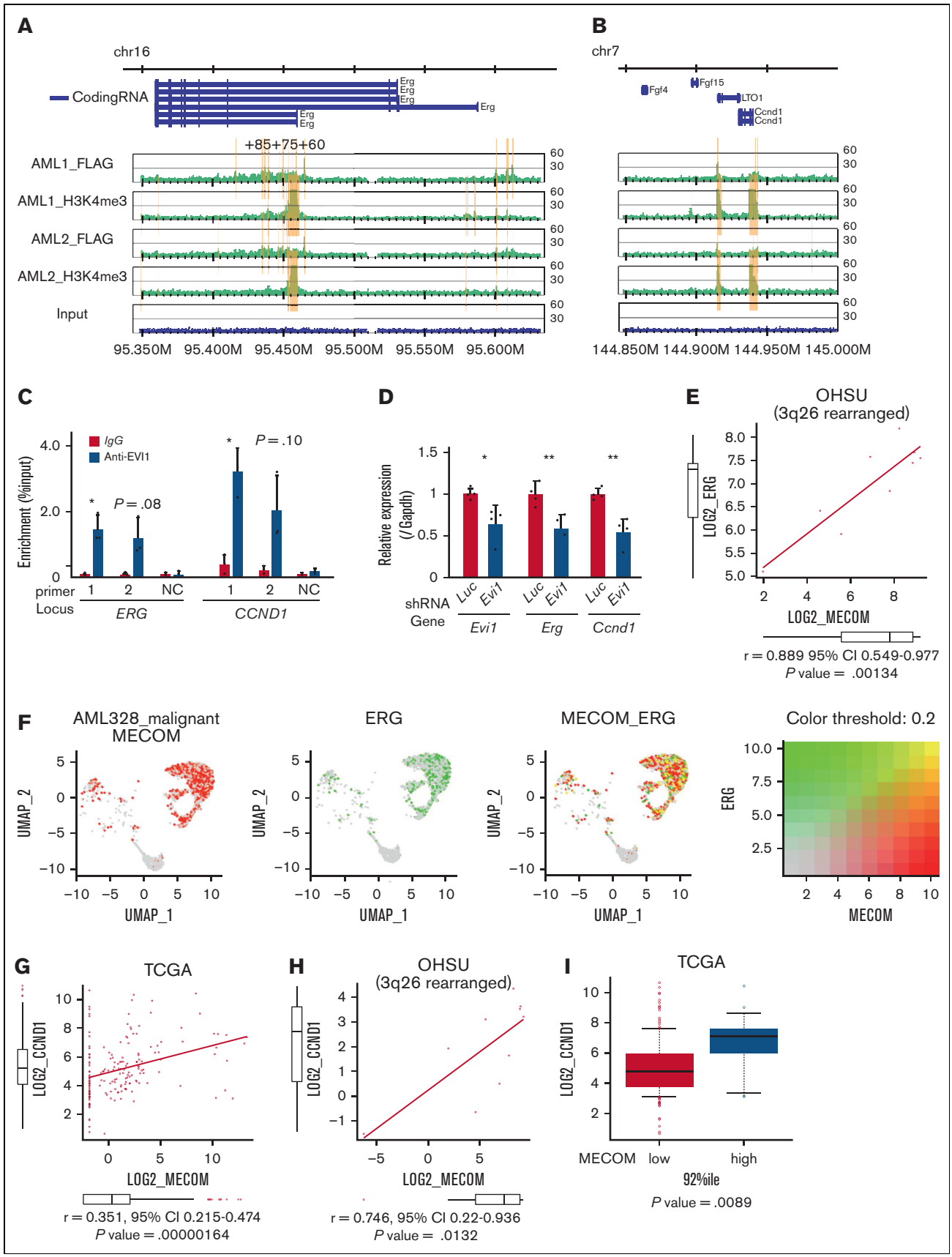

Figure 3.

(supplemental Figure 4K). These findings suggest that ERG is necessary to maintain a transformed phenotype of EVI1$^+$ AML.

Genes involved in the ribosomal process are enriched in genes associated with ERG

We performed RNA-seq using EVI1-AML cells after the transduction of sh*Erg*. When we compared the differentially regulated genes in our AML models with those in normal HSCs after deletion of *Erg*,[21] there was no apparent correlation (supplemental Figure 4L). In addition, the fact that a relatively small number of genes were differentially expressed in our AML model and that MYC target genes were downregulated after *Erg* knockdown, in contrast to the upregulation after *Erg* deletion in normal HSCs,[21] led us to search for genes regulated by ERG in an AML-specific manner (supplemental Figure 4M-N). The RNA-seq revealed that ribosome-related processes are enriched in downregulated genes upon *Erg* knockdown (Figure 4J-K). Using publicly available anti-ERG ChIP-seq data of human hematopoietic cells,[27,64-66] we identified genes involved in translation and ribosomal formation as possible differentially binding regions of ERG between normal cells and AML cell lines (supplemental Figure 4O). Along with these findings, gene expression correlation analysis using the human AML data set revealed that gene sets associated with ribosomes and translation were also identified as genes whose expression levels correlate with ERG (supplemental Figure 4P).

Cyclin D1 plays a key role in murine *EVI1*$^+$ AML models

Despite the established multihued functions of cyclin D1 in several malignancies,[67] its role in AML is poorly understood. Silencing of *Ccnd1* in EVI1-AML cells decreased in vitro proliferation with marginal cell cycle delay (Figure 5A and supplemental Figure 5A-C). Knockdown of *Ccnd1* also inhibited the colony-forming activity, indicating the functional needs in EVI1-AML (Figure 5B). KMT2A-MLLT1 CL2 cells were mildly dependent on cyclin D1, whereas CL1 was not (Figure 5C-D and supplemental Figure 5D-E). *Ccnd1* silencing did not affect MOZ-TIF2 and HOXA9-MEIS1 AML cells (supplemental Figure 5F). These cells also showed different sensitivity to pharmacological inhibition of CDK4/CDK6 with palbociclib and fascaplysin (supplemental Figure 5G-I).

We assessed the effect of *Ccnd1* silencing on the leukemogenic potential of EVI1-AML cells in vivo. Although homing to the BM was not affected by *Ccnd1* silencing, the frequency of GFP$^+$ EVI1-AML cells in the peripheral blood expressing shRNAs against *Ccnd1* was lower 4 weeks after transplantation (Figure 5E and supplemental Figure 5J). Development of EVI1 and KMT2A-MLLT1 AML was hampered by *Ccnd1* knockdown (Figure 5F-G). These data suggest that cyclin D1 plays a vital role in AML development in murine *EVI1*$^+$ AML models.

Cyclin D1 is associated with IFN signatures and immune exhaustion in EVI1-AML

To explore downstream processes of cyclin D1, RNA-seq analysis using EVI1-AML cells was performed after transduction of sh*Ccnd1*. Surprisingly, silencing of *Ccnd1* led to downregulation of genes associated with chemokine production and response to IFN instead of cell cycle–related genes (Figure 6A and supplemental Figure 6A-C). In RNA-seq of the c-kit$^+$ fraction of AML cells freshly isolated from EVI1-AML mice expressing shRNAs, gene set enrichment analysis also demonstrated that gene sets associated with chemokine and IFN were downregulated in sh*Ccnd1* cells (Figure 6B and supplemental Figure 6D). The expression of *Stat1*, the primary signaling mediator for type I and II IFN, was decreased in cells with sh*Ccnd1* (Figure 6C). Intriguingly, it has been suggested that EVI1 may directly upregulate STAT1.[68] In addition to the decrease in *Stat1* mRNA after *Evi1* knockdown, the reporter assay suggested that EVI1 upregulates STAT1 through direct mechanisms as well (supplemental Figure 6E-G). As IFN-γ has been implicated in promoting the immunosuppressive tumor microenvironment, T cells from sh*Ccnd1* EVI1-AML mice were analyzed for expression of exhaustion markers. Spleen T cells from the secondary EVI1-AML recipients on day 19, engrafted with freshly isolated sh*Ccnd1* EVI1-AML cells, showed decreased expression of molecules associated with exhaustion, including *Lag3*, *Pdcd1,* and *Tigit* (Figure 6D and supplemental Figure 6H). CD4 and CD8 T cells infiltrating the liver from sh*Ccnd1* EVI1-AML mice also demonstrated lower positivity of PDCD1 and TIGIT, suggesting a role of cyclin D1 expressed by AML cells in T-cell exhaustion (Figure 6E-F and supplemental Figure 6I). To confirm the validity of our findings, we assessed whether the relationship found in our murine AML models was also observed in human AML by utilizing public gene expression data.[51,52] IFN-γ score, as a substitute indicator for IFN-γ level,[44] was positively correlated with *MECOM* and *CCND1*, whereas *CCND1* was more strongly correlated (Figure 6G-H and supplemental Figure 6J-K). The expressions of *STAT1* and *CD274*, an immune checkpoint molecule regulated by the IFN pathway and also known as PD-L1, were also positively correlated to those of *MECOM* and *CCND1* (Figure 6I-J and supplemental Figure 6L-N).

IFN-γ and STAT1 axis plays a crucial role in the development of EVI1-AML

In agreement with the reported antitumor activity of STAT1 as a general rule,[69] silencing of *Stat1* in EVI1-AML cells did not affect in vitro proliferation (supplemental Figure 7A-B). However, knockdown of *Stat1* or *Ifngr*, the receptor of IFN-γ, substantially impaired the leukemogenic capacity of EVI1-AML in vivo (Figure 7A-B), whereas silencing of *Ifnar*, the receptor of IFN-α/β, had no effect

Figure 3. ERG and CCND1 are targets of EVI1 in *Evi1*^{high} AML cells. (A-B) Illustration of anti-FLAG and anti-H3K4me3 ChIP-seq results for FLAG-tagged EVI1 in the murine *Erg* locus around the alternative transcription start site (A) and the murine *Ccnd1* promoter region (B). Yellow bars represent significantly enriched regions. (C) ChIP-qPCR analysis using anti-EVI1 antibody and HNT-34 AML cells showing the binding of EVI1 to the corresponding human regions identified in the ChIP-seq of the murine EVI1-AML samples. Neighborhood sequences without enrichment in the ChIP-seq were used as a negative control. (D) qPCR showing the relative expression of *Evi1*, *Erg,* and *Ccnd1* in EVI1-AML cells expressing shRNA against *Evi1*. (E) Gene expression correlation analysis between *MECOM* and *ERG* in Oregon Health Sciences University (OHSU) AML cohorts with 3q26 abnormalities. (F) A 2-color dot plot showing coexpression of *MECOM* and *ERG* in the scRNA-seq data from a patient with AML (AML328). (G) Gene expression correlation analysis between *MECOM* and *CCND1* in The Cancer Genome Atlas (TCGA) AML cohorts. (H) Gene expression correlation analysis between *MECOM* and *CCND1* in OHSU AML cohorts with 3q26 abnormalities. (I) A box plot showing *CCND1* expression in TCGA *EVI1*$^+$ and *EVI1*$^-$ AML cohorts. Mean ± SD. *$P < .05$, **$P < .01$.

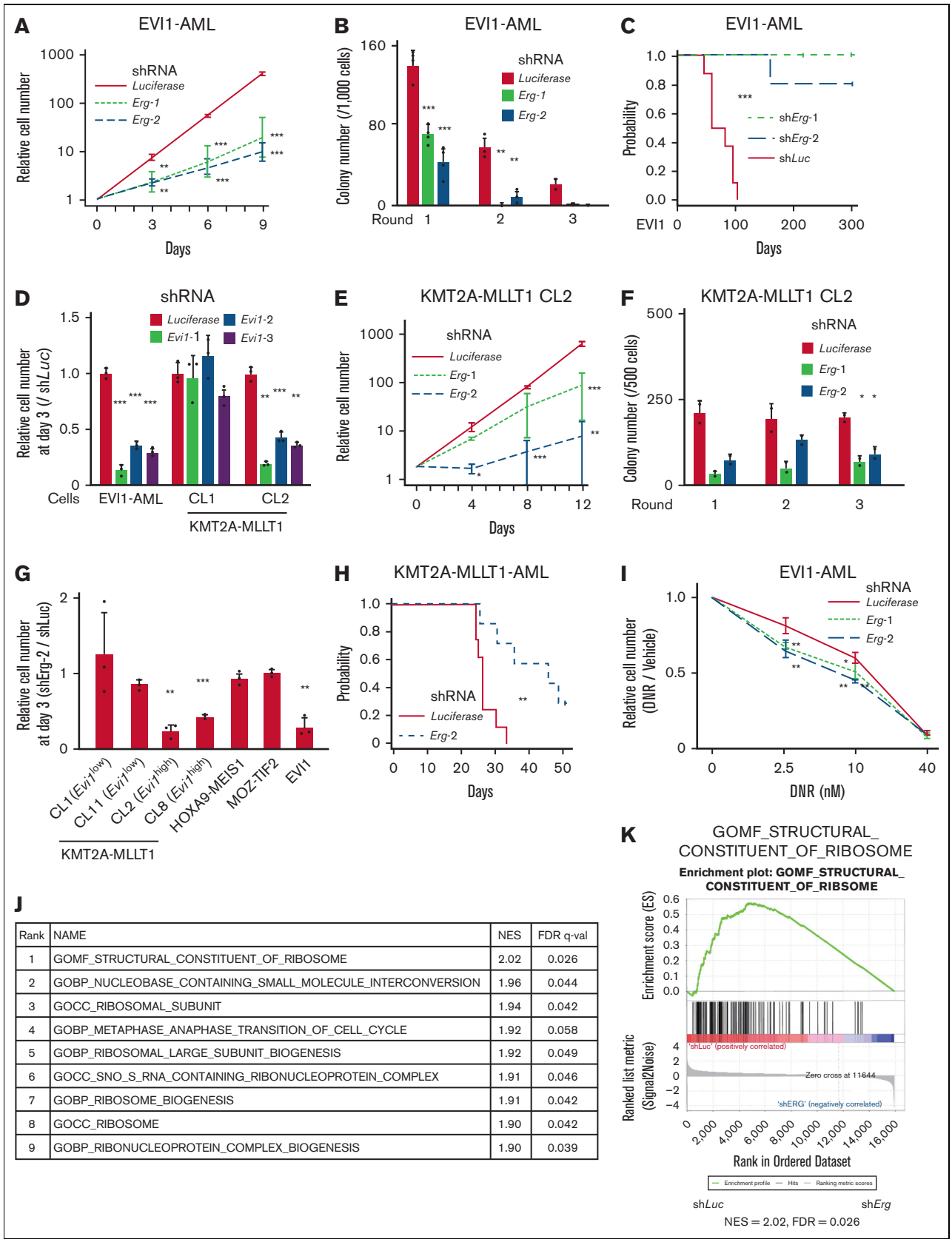

J

Rank	NAME	NES	FDR q-val
1	GOMF_STRUCTURAL_CONSTITUENT_OF_RIBOSOME	2.02	0.026
2	GOBP_NUCLEOBASE_CONTAINING_SMALL_MOLECULE_INTERCONVERSION	1.96	0.044
3	GOCC_RIBOSOMAL_SUBUNIT	1.94	0.042
4	GOBP_METAPHASE_ANAPHASE_TRANSITION_OF_CELL_CYCLE	1.92	0.058
5	GOBP_RIBOSOMAL_LARGE_SUBUNIT_BIOGENESIS	1.92	0.049
6	GOCC_SNO_S_RNA_CONTAINING_RIBONUCLEOPROTEIN_COMPLEX	1.91	0.046
7	GOBP_RIBOSOME_BIOGENESIS	1.91	0.042
8	GOCC_RIBOSOME	1.90	0.042
9	GOBP_RIBONUCLEOPROTEIN_COMPLEX_BIOGENESIS	1.90	0.039

Figure 4. *Evi1*^{high} AML cells are dependent on ERG. (A) Relative cell proliferation of EVI1-AML cells expressing shRNAs against *Luciferase* and *Erg* in vitro. (B) Colony-forming units of EVI1-AML cells expressing shRNAs against *Luciferase* and *Erg*. (C) A Kaplan-Meier survival curve for recipient mice that underwent transplantation with 1 × 10^6

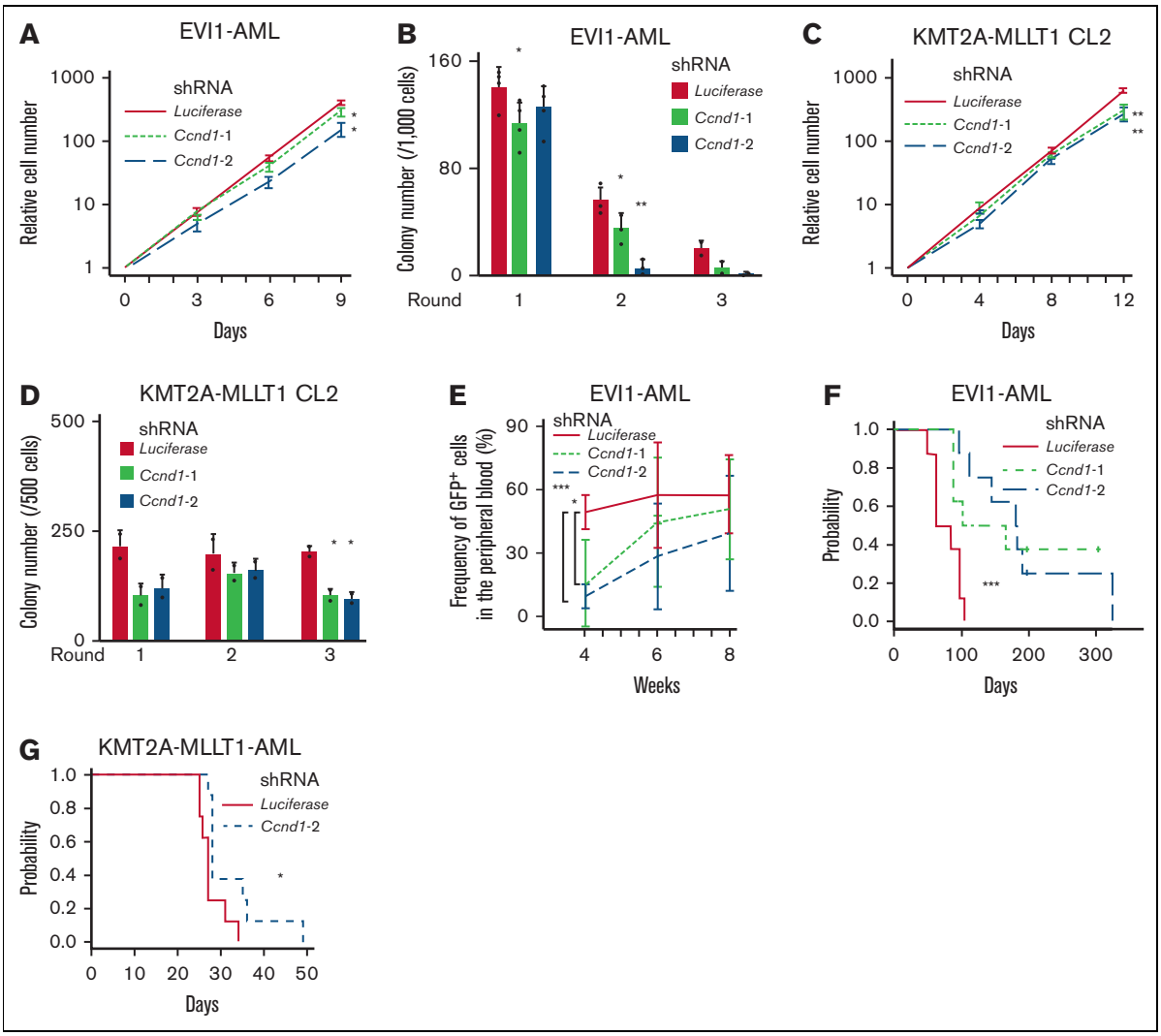

Figure 5. Cyclin D1 is necessary for the efficient development of EVI1-AML in vivo. (A) Relative cell proliferation of EVI1-AML cells expressing shRNAs against *Luciferase* and *Ccnd1* in vitro. The data for sh*Luciferase* are common to those in Figure 4A. (B) Colony-forming units of EVI1-AML cells expressing shRNAs against *Luciferase* and *Ccnd1*. The data for sh*Luciferase* are common to those in Figure 4B. (C) Relative cell proliferation of KMT2A-MLLT1 CL2 cells expressing shRNAs against *Luciferase* and *Ccnd1* in vitro. The data for sh*Luciferase* are common to Figure 4E. (D) Colony-forming units of KMT2A-MLLT1 CL2 cells expressing shRNAs against *Luciferase* and *Ccnd1*. The data for sh*Luciferase* are common to Figure 4F. (E) Frequency of GFP^+ AML cells in the peripheral blood in recipient mice that underwent transplantation with EVI1-AML cells expressing indicated shRNAs. (F) A Kaplan-Meier survival curve for recipient mice that underwent transplantation with 1×10^6 EVI1-AML cells expressing shRNAs against *Luciferase* and *Ccnd1*, after being exposed to 6.5 Gy TBI. *P* value was examined by a log-rank test. The data for sh*Luciferase* are common to Figure 4C. (G) A Kaplan-Meier survival curve for recipient mice that underwent transplantation with 1×10^4 KMT2A-MLLT1-AML cells expressing shRNAs against *Luciferase* and *Ccnd1,* after being exposed to 6.5 Gy TBI. *P* value was examined by a log-rank test. The data for sh*Luciferase* are common to Figure 4H. Mean ± SD. $^*P < .05$, $^{**}P < .01$, $^{***}P < .001$.

Figure 4 (continued) EVI1-AML cells expressing shRNAs against *Luciferase* and *Erg* after being exposed to 6.5 Gy TBI. *P* value was examined by a log-rank test. (D) Relative cell proliferation of EVI1-AML and KMT2A-MLLT1 clone 1 (CL1) and CL2 cells expressing shRNAs against *Luciferase* and *Evi1* in vitro, showing EVI1-dependency of these cells. (E) Relative cell proliferation of KMT2A-MLLT1 CL2 cells expressing shRNAs against *Luciferase* and *Erg* in vitro. (F) Colony-forming units of KMT2A-MLLT1 CL2 cells expressing shRNAs against *Luciferase* and *Erg*. (G) Relative cell proliferation of several AML cells and KMT2A-MLLT1-transformed cell lines with sh*Erg* compared with those with sh*Luciferase*, through days 0 to 3. A comparison was made within the same original cell between sh*Luciferase* and sh*Erg*. (H) A Kaplan-Meier survival curve for recipient mice that underwent transplantation with 1×10^4 KMT2A-MLLT1 AML cells expressing shRNAs against *Luciferase* and *Erg* after being exposed to 6.5 Gy TBI. (I) Relative live cell numbers of EVI1-AML cells with shRNAs against *Luciferase* or *Erg* treated with daunomycin, compared with those cultured in media without daunomycin. (J) A list of top-ranked gene sets with decreased expression in sh*Erg*-transduced EVI1-AML cells. (K) GSEA showing structural constituent of the ribosome is downregulated in sh*Erg*. Mean ± SD; $^*P < .05$, $^{**}P < .01$, $^{***}P < .001$.

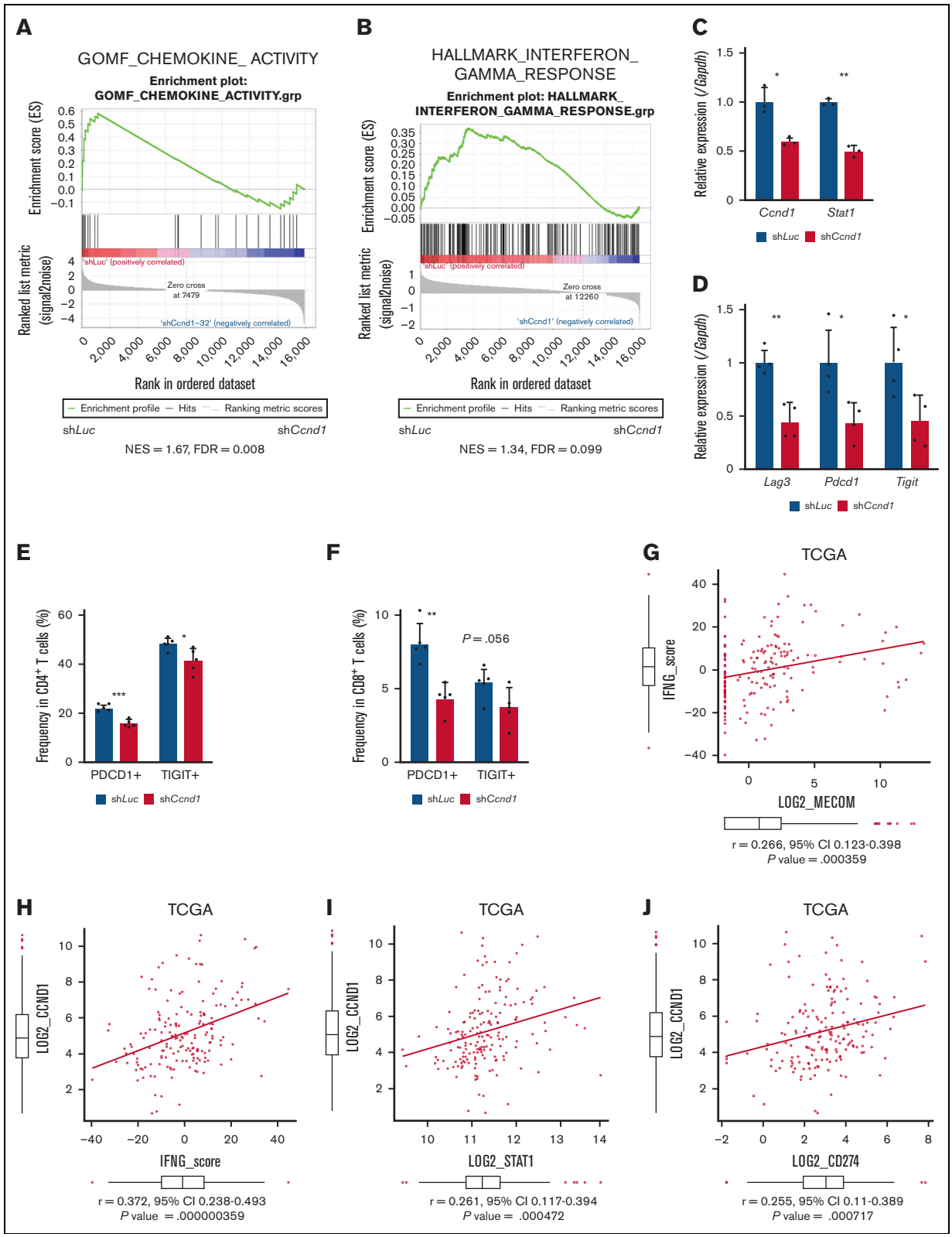

Figure 6. Cyclin D1 is associated with IFN signatures and immune exhaustion in EVI1-AML. (A) GSEA showing that gene sets associated with chemokine activity are downregulated after silencing *Ccnd1* in vitro. (B) GSEA showing that gene sets associated with IFN-γ signaling are upregulated by silencing *Ccnd1* in vivo. (C) qPCR showing the relative expression of *Stat1* in EVI1-AML cells with *Ccnd1* silencing. (D) qPCR showing the relative expression of exhaustion-related genes in the spleen T cells from sh*Luc*- or sh*Ccnd1*-EVI1-AML mice before the development of full-blown AML. Freshly isolated AML cells (1×10^6) from sh*Luc*- or sh*Ccnd1*-EVI1-AML mice were injected into the

(supplemental Figure 7C-E). Knockdown of *Ifngr* and *Stat1*, but not *Ifnar*, also decreased the expression of exhaustion-related molecules such as PDCD1 and TIGIT on T and natural killer (NK) cells (Figure 7C-E). In other AML models, including HOXA9-MEIS1 and KMT2A-MLLT1 without EVI1 expression, silencing of *Ifngr* and *Stat1* did not affect exhaustion phenotype or survival (data not shown), suggesting the specificity of EVI1-AML. These results collectively suggest the vital role of the IFN-γ/STAT1 pathway in the immunosuppressive tumor microenvironment and the development of EVI1-AML.

Because AML cells do not express *Ifng*, we collected $CD3^+$ T and $CD49b^+$ NK cells from the spleen and found that the expression of *Ifng* in T cells and NK cells was reduced in mice engrafted with sh*Ccnd1*-EVI1-AML cells (Figure 7F). As *Ccnd1* silencing was associated with decreased cytokine production in EVI1-AML cells (Figure 6A) and various chemokines have been implicated in the recruitment of IFN-γ–producing effector cells to the tumor microenvironment,[70,71] we determined the expression of specific chemokines reported to be involved in the process. qPCR, after silencing *Ccnd1* in EVI1-AML cells, also demonstrated markedly reduced expression of chemokines, including *Ccl2*, *Ccl4*, and *Ccl5* (Figure 7G). Intriguingly, in vitro treatment of EVI1-AML cells by palbociclib, where the proliferation was inhibited as much as genetic silencing of *Ccnd1*, the expression of chemokines and *Stat1* was not affected (supplemental Figure 7F). Together with the modest difference in the sensitivity to CDK4/6 inhibitors between cells with different EVI1 expression in vitro (supplemental Figure 5G-I), the only partial recapitulation of the effect of silencing *Ccnd1* by pharmacological inhibition of CDK4/6 might suggest the multifaceted roles of cyclin D1, including both CDK4/CDK6-dependent and independent ones.

We validated our findings using human AML data sets to find that high expressions of *CCL4* and *CCL5* were associated with inferior survival, indicating the functional importance of these chemokines (Figure 7H-I). The expression of *CCL2* and *CCL4* was also positively correlated to those of *MECOM* and *CCND1* (Figure 7J and supplemental Figure 7G-I). Using CIBERSORTx on these data, a computational framework to infer cell-type–specific gene expression,[55] we estimated the association between specific gene expressions in immune cells and bulk expressions of *MECOM* and *CCND1*. Positive correlations were seen with *TIGIT* in CD4 and CD8 T cells, a checkpoint receptor involved in T-cell exhaustion, and *IFNG* in CD8 T cells as expected (Figure 7K-M and supplemental Figure 7J-L). The expression of costimulatory receptor *ICOS* in CD8 T cells was negatively related to those of *MECOM* and *CCND1* (Figure 7N and supplemental Figure 7M). *LAG3* in NK cells was also positively correlated with *MECOM* and *CCND1* (Figure 7O and supplemental Figure 7N). These data were consistent with the immunoinhibitory functions of MECOM and cyclin D1 in human AML.

Discussion

This study identified ERG and cyclin D1 as potential targets of EVI1 by using murine $EVI1^+$ AML models. $EVI1^+$ AML is known to be highly resistant to cytotoxic chemotherapy and associated with a very poor prognosis. The results of this study may provide potential therapeutic targets for this type of disease.

Given the intercellular heterogeneity of *EVI1* expression, we compared the properties of EVI1-GFP-high and -low cells. The aggressive behavior of $Evi1^{high}$ cells is consistent with the results of previous studies.[72,73] Although the diversity of GFP^{high} cells in their clonogenic ability may reflect the heterogeneity of the LSK fraction used to generate the model, it is of particular interest that EVI1-GFP^{high} cells were not associated with stemness. Furthermore, our analysis showed that the *Evi1* expression was associated with differences in the properties of AML cells on a cell basis, including leukemogenic potential and persistence after chemotherapy. $Evi1^{high}$ cells expressed a higher level of *Erg* and associated gene expression profiles, and EVI1-AML cells became more sensitive to chemotherapy upon *Erg* knockdown, suggesting the functional involvement of EVI1 and ERG in $EVI1^+$ AML.

This study showed that ERG was requisite in murine $EVI1^+$ AML, like HSCs.[21] There was, however, little overlap in genes regulated by ERG between normal HSCs and EVI1-AML cells, collectively suggesting that ERG plays a distinct role in AML. Supporting our findings, a complementary article by Schmöllerl et al has identified ERG as an important transcriptional target of EVI1 through characterizing chromatin binding of Evi1 and transcriptional profiling in a human AML model.[74] The role of ERG in regulating the ribosomal process and its implication in EVI1-AML should be investigated in future studies.

In this study, we present a novel mechanism of immune exhaustion mediated by cyclin D1. Although analysis of the direct transcriptional regulation by cyclin D1 has only just begun,[31,32] the binding of cyclin D1 to multiple chemokine loci including *CCL4* and upregulation of *CCL2* has been demonstrated,[75] in agreement with our data. Because the expression of multiple chemokines seems to be controlled in parallel by cyclin D1, and it has been known to be activated by IFN-signaling itself, further studies are needed to determine what role chemokines play in the formation of IFN signature. Silencing *Ccnd1* in EVI1-AML cells in vitro also attenuated IFN-signature, suggesting additional mechanisms might be working to regulate IFN signaling, such as a direct, cell-intrinsic effect. In addition, pharmacological inhibition of CDK4/6 only partially recapitulated the effect of silencing *Ccnd1*, suggesting a CDK4/6-independent role for cyclin D1. Considering that CDK4/6 inhibition enhances antitumor immunity in solid cancers via multiple mechanisms,[34-36,52] the function of cyclin D1 seems diverse. In addition, given that EVI1 has different effects on the IFN pathway and that it has been suggested that EVI1 may be a direct target of STAT1 in a previous report and our

Figure 6 (continued) secondary recipient mice without TBI, followed by T-cell isolation from the spleen 19 days after transplant. Please see supplemental Figure 6H. (E) Frequency of cellular subsets of CD4 T cells infiltrating the liver of EVI1-AML mice with frank leukemia. Please see supplemental Figure 6I. (F) Frequency of cellular subsets of CD8 T cells infiltrating the liver of EVI1-AML mice with indicated shRNA after exposure to 4.5 Gy TBI. Please see supplemental Figure 6I. (G-H) Pearson correlation analysis between IFN-γ score and *MECOM*/*CCND1* expression in TCGA samples. (I) Pearson correlation analysis between *STAT1* and *CCND1* expression in TCGA samples. (J) Pearson correlation analysis between *CD274* and *CCND1* expression in TCGA samples. Mean ± SD. $^*P < .05$, $^{**}P < .01$, $^{***}P < .001$.

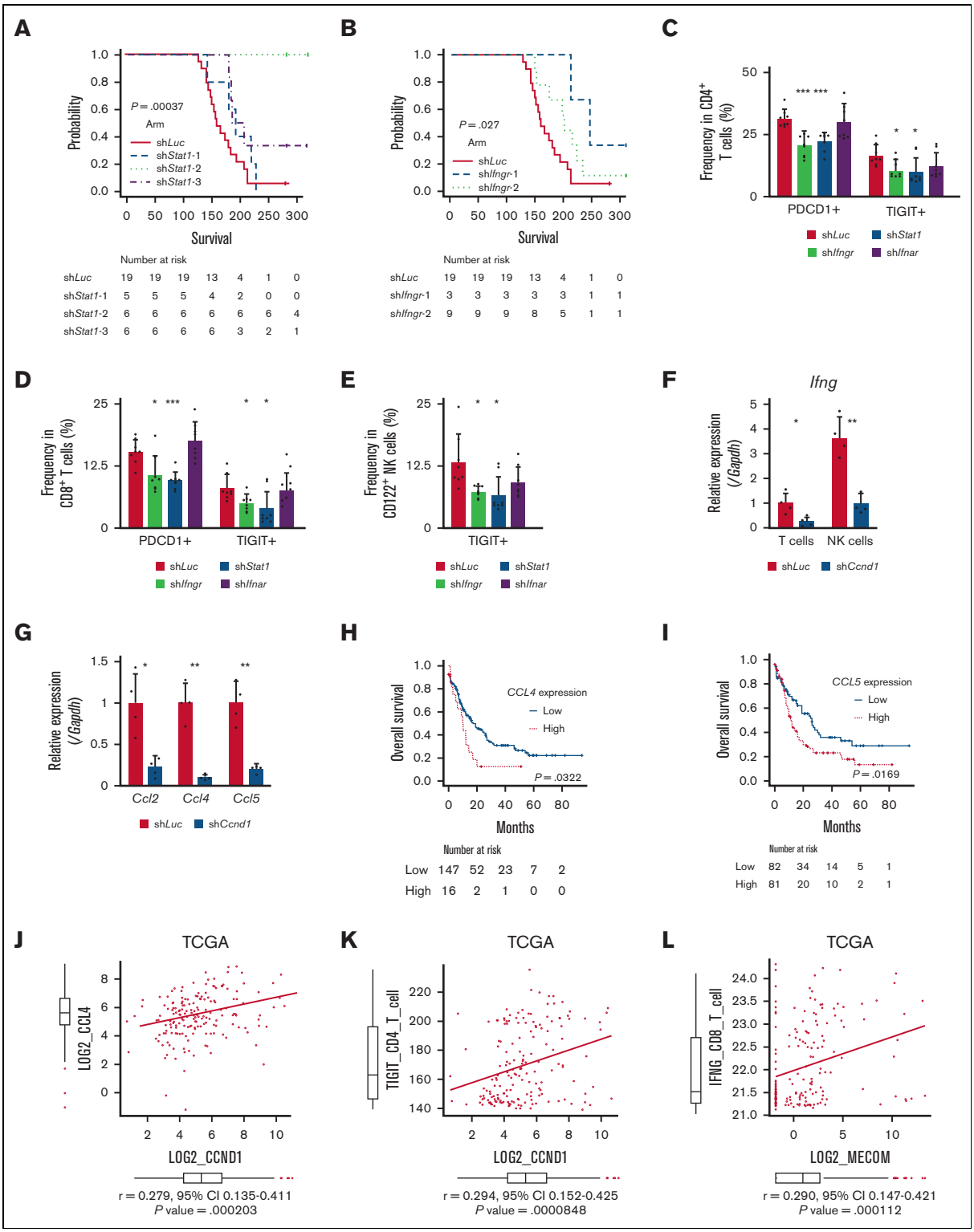

Figure 7. Overexpression of *CCND1* is associated with type II IFN signature in human AML. (A-B) A Kaplan-Meier survival curve for recipient mice that underwent transplantation with 1 × 10^6 EVI1-AML cells expressing shRNAs against indicated genes, after exposure to 4.5 Gy TBI. The data for sh*Luciferase* are common in Figure 7A-B and supplemental Figure 7E. (C-E) Frequency of cellular subsets of CD4 T (C), CD8 T (D), and CD122$^+$ NK (E) cells infiltrating the spleen of EVI1-AML mice with indicated shRNA after exposure to 6.5 Gy TBI. Please see supplemental Figure 6H. (F) qPCR showing the relative expression of *Ifng* in the spleen T and NK cells from sh*Luc*- or sh*Ccnd1*-EVI1-AML mice, used in Figure 6D. (G) qPCR showing the relative expression of chemokines in the EVI1-AML cells 72 hours after transduction of sh*Luc* or sh*Ccnd1*. (H) An overall survival of TCGA cohorts according to *CCL4* expression divided at 90th percentile. (I) Overall survival of TCGA cohorts according to *CCL5* expression divided at

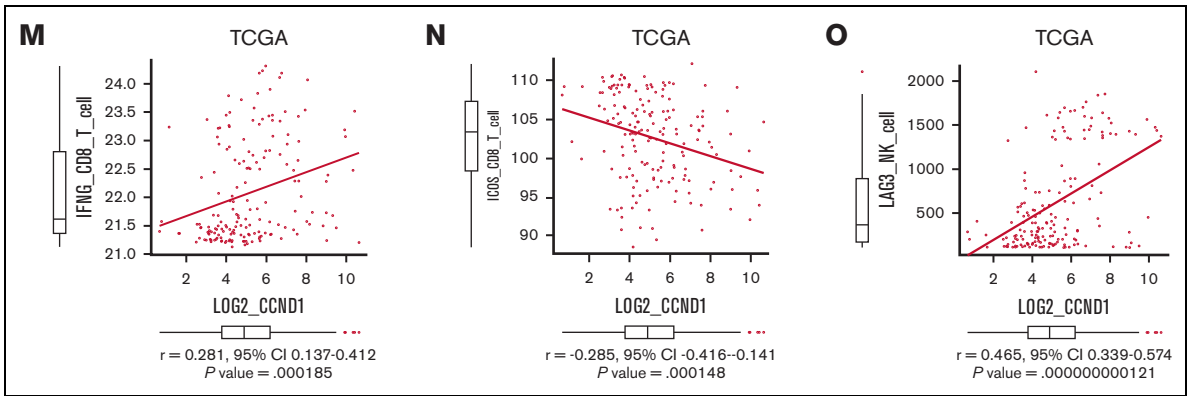

Figure 7 (continued) 50th percentile. (J) Pearson correlation analysis between *CCL4* and *CCND1* expression in TCGA samples. (K) Pearson correlation analysis between estimated expression *of TIGIT* in CD4 T cells calculated using CIBERSORTx and *CCND1* expression in TCGA samples. (L-M) Pearson correlation analysis between estimated expression of *IFNG* in CD8 T cells calculated using CIBERSORTx and *MECOM*/*CCND1* expressions in TCGA samples. (N) Pearson correlation analysis between estimated expression *of ICOS* in CD8 T cells calculated using CIBERSORTx and *CCND1* expression in TCGA samples. (O) Pearson correlation analysis between estimated expression of *LAG3* in NK cells calculated using CIBERSORTx and *CCND1* expression in TCGA samples. Mean ± SD. $*P < .05$, $**P < .01$, $***P < .001$.

ChIP-seq, further studies are needed to elucidate the full picture of the relationship between EVI1, CCND1, and the IFN-γ pathway.[68,76]

The impact of immune biology on the pathogenesis of AML has received increasing attention. In AML with immune cell infiltration, IFN-γ–related transcriptional profiles are associated with immune exhaustion and chemoresistance, of which the molecular bases are unclear.[45] TP53 mutations are associated with immune cell infiltration,[77] and ASXL1 mutations induce T-cell exhaustion.[78] Although there might be a role of immune evasion as the basis for refractoriness, the mechanisms might be different between subtypes. Our study provides a possible mechanism of immune evasion in *EVI1*$^+$ AML through cyclin D1.

Although model-dependent differences in EVI1 expression levels might affect the results, this work demonstrated that EVI1 confers AML cells with dependency on ETS transcription factor ERG and immunoregulatory capacity in the tumor microenvironment through cyclin D1, both of which can be therapeutic vulnerabilities of *EVI1*$^+$ AML cells.

Acknowledgments

The authors thank T. Kitamura for PLAT-E packaging cells and K. Ono, K. Higa, and M. Ebisawa for expert technical assistance. The authors thank Johannes Zuber and Johannes Schmolellerl for their scientific discussions and for sharing unpublished data and manuscripts.

This work was partly supported by the Japan Society for the Promotion of Science KAKENHI (JP20H03708 and JP21H04805) and a scholarship from Kyowa Kirin.

Authorship

Contribution: Y.M., A.C., and M.K. conceptualized the study; Y.M. and M.K. developed the study methodology; Y.M., A.C., H.M., and M.B. performed investigation; Y.M., T.S., and M.K. provided resources; Y.M. wrote the original draft; Y.M., A.C., H.M., T.H., H.H., T.S., M.B., K.S., and M.K. wrote, reviewed, and edited the manuscript; Y.M. and M.K. acquired funding; and M.K. performed study supervision.

Conflict-of-interest disclosure: The authors declare no competing financial interest.

ORCID profiles: Y.M., 0000-0002-8168-6459; T.S., 0000-0002-8244-075X; M.B., 0000-0003-4852-1625; K.S., 0000-0002-7862-1144; M.K., 0000-0002-4034-2422.

Correspondence: Mineo Kurokawa, Department of Hematology & Oncology, Graduate School of Medicine, The University of Tokyo, 7-3-1 Hongo, Bunkyo-Ku, Tokyo 113-8655, Japan; email: kurokawa@m.u-tokyo.ac.jp.

References

1. Döhner H, Weisdorf DJ, Bloomfield CD. Acute myeloid leukemia. *N Engl J Med*. 2015;373(12):1136-1152.
2. DiNardo CD, Stein EM, de Botton S, et al. Durable remissions with ivosidenib in IDH1-mutated relapsed or refractory AML. *N Engl J Med*. 2018;378(25):2386-2398.
3. Perl AE, Martinelli G, Cortes JE, et al. Gilteritinib or chemotherapy for relapsed or refractory FLT3-mutated AML. *N Engl J Med*. 2019;381(18):1728-1740.
4. DiNardo CD, Schuh AC, Stein EM, et al. Enasidenib plus azacitidine versus azacitidine alone in patients with newly diagnosed, mutant-IDH2 acute myeloid leukaemia (AG221-AML-005): a single-arm, phase 1b and randomised, phase 2 trial. *Lancet Oncol*. 2021;22(11):1597-1608.

5. Morishita K, Parker DS, Mucenski ML, Jenkins NA, Copeland NG, Ihle JN. Retroviral activation of a novel gene encoding a zinc finger protein in IL-3-dependent myeloid leukemia cell lines. *Cell*. 1988;54(6):831-840.
6. Buonamici S, Li D, Chi Y, et al. EVI1 induces myelodysplastic syndrome in mice. *J Clin Invest*. 2004;114(5):713-719.
7. Jin G, Yamazaki Y, Takuwa M, et al. Trib1 and Evi1 cooperate with Hoxa and Meis1 in myeloid leukemogenesis. *Blood*. 2007;109(9):3998-4005.
8. Yoshimi A, Goyama S, Watanabe-Okochi N, et al. Evi1 represses PTEN expression and activates PI3K/AKT/mTOR via interactions with polycomb proteins. *Blood*. 2011;117(13):3617-3628.
9. Valk PJ, Verhaak RG, Beijen MA, et al. Prognostically useful gene-expression profiles in acute myeloid leukemia. *N Engl J Med*. 2004;350(16):1617-1628.
10. Gröschel S, Lugthart S, Schlenk RF, et al. High EVI1 expression predicts outcome in younger adult patients with acute myeloid leukemia and is associated with distinct cytogenetic abnormalities. *J Clin Oncol*. 2010;28(12):2101-2107.
11. Yamazaki H, Suzuki M, Otsuki A, et al. A remote GATA2 hematopoietic enhancer drives leukemogenesis in inv(3)(q21;q26) by activating EVI1 expression. *Cancer Cell*. 2014;25(4):415-427.
12. Gröschel S, Sanders MA, Hoogenboezem R, et al. A single oncogenic enhancer rearrangement causes concomitant EVI1 and GATA2 deregulation in leukemia. *Cell*. 2014;157(2):369-381.
13. Katayama S, Suzuki M, Yamaoka A, et al. GATA2 haploinsufficiency accelerates EVI1-driven leukemogenesis. *Blood*. 2017;130(7):908-919.
14. Yamaoka A, Suzuki M, Katayama S, Orihara D, Engel JD, Yamamoto M. EVI1 and GATA2 misexpression induced by inv(3)(q21q26) contribute to megakaryocyte-lineage skewing and leukemogenesis. *Blood Adv*. 2020;4(8):1722-1736.
15. Ottema S, Mulet-Lazaro R, Beverloo HB, et al. Atypical 3q26/MECOM rearrangements genocopy inv(3)/t(3;3) in acute myeloid leukemia. *Blood*. 2020;136(2):224-234.
16. Hoyt PR, Bartholomew C, Davis AJ, et al. The Evi1 proto-oncogene is required at midgestation for neural, heart, and paraxial mesenchyme development. *Mech Dev*. 1997;65(1-2):55-70.
17. Goyama S, Yamamoto G, Shimabe M, et al. Evi-1 is a critical regulator for hematopoietic stem cells and transformed leukemic cells. *Cell Stem Cell*. 2008;3(2):207-220.
18. Fenouille N, Bassil CF, Ben-Sahra I, et al. The creatine kinase pathway is a metabolic vulnerability in EVI1-positive acute myeloid leukemia. *Nat Med*. 2017;23(3):301-313.
19. Mizuno H, Koya J, Masamoto Y, Kagoya Y, Kurokawa M. Evi1 upregulates Fbp1 and supports progression of acute myeloid leukemia through pentose phosphate pathway activation. *Cancer Sci*. 2021;112(10):4112-4126.
20. Ng AP, Loughran SJ, Metcalf D, et al. Erg is required for self-renewal of hematopoietic stem cells during stress hematopoiesis in mice. *Blood*. 2011;118(9):2454-2461.
21. Knudsen KJ, Rehn M, Hasemann MS, et al. ERG promotes the maintenance of hematopoietic stem cells by restricting their differentiation. *Genes Dev*. 2015;29(18):1915-1929.
22. Baldus CD, Burmeister T, Martus P, et al. High expression of the ETS transcription factor ERG predicts adverse outcome in acute T-lymphoblastic leukemia in adults. *J Clin Oncol*. 2006;24(29):4714-4720.
23. Marcucci G, Maharry K, Whitman SP, et al. High expression levels of the ETS-related gene, ERG, predict adverse outcome and improve molecular risk-based classification of cytogenetically normal acute myeloid leukemia: a Cancer and Leukemia Group B Study. *J Clin Oncol*. 2007;25(22):3337-3343.
24. Tsuzuki S, Taguchi O, Seto M. Promotion and maintenance of leukemia by ERG. *Blood*. 2011;117(14):3858-3868.
25. Chen X, Qin Y, Zhang Z, et al. Hyper-SUMOylation of ERG is essential for the progression of acute myeloid leukemia. *Front Mol Biosci*. 2021;8:652284.
26. Huang Y, Sitwala K, Bronstein J, et al. Identification and characterization of Hoxa9 binding sites in hematopoietic cells. *Blood*. 2012;119(2):388-398.
27. Martens JH, Mandoli A, Simmer F, et al. ERG and FLI1 binding sites demarcate targets for aberrant epigenetic regulation by AML1-ETO in acute myeloid leukemia. *Blood*. 2012;120(19):4038-4048.
28. Yoshino S, Yokoyama T, Sunami Y, et al. Trib1 promotes acute myeloid leukemia progression by modulating the transcriptional programs of Hoxa9. *Blood*. 2021;137(1):75-88.
29. Kato J, Matsushime H, Hiebert SW, Ewen ME, Sherr CJ. Direct binding of cyclin D to the retinoblastoma gene product (pRb) and pRb phosphorylation by the cyclin D-dependent kinase CDK4. *Genes Dev*. 1993;7(3):331-342.
30. Lundberg AS, Weinberg RA. Functional inactivation of the retinoblastoma protein requires sequential modification by at least two distinct cyclin-cdk complexes. *Mol Cell Biol*. 1998;18(2):753-761.
31. Bienvenu F, Jirawatnotai S, Elias JE, et al. Transcriptional role of cyclin D1 in development revealed by a genetic-proteomic screen. *Nature*. 2010;463(7279):374-378.
32. Casimiro MC, Crosariol M, Loro E, et al. ChIP sequencing of cyclin D1 reveals a transcriptional role in chromosomal instability in mice. *J Clin Invest*. 2012;122(3):833-843.
33. Chen Y, Huang Y, Gao X, et al. CCND1 amplification contributes to immunosuppression and is associated with a poor prognosis to immune checkpoint inhibitors in solid tumors. *Front Immunol*. 2020;11:1620.
34. Goel S, DeCristo MJ, Watt AC, et al. CDK4/6 inhibition triggers anti-tumour immunity. *Nature*. 2017;548(7668):471-475.

35. Heckler M, Ali LR, Clancy-Thompson E, et al. Inhibition of CDK4/6 promotes CD8 T-cell memory formation. *Cancer Discov*. 2021;11(10):2564-2581.

36. Lelliott EJ, Kong IY, Zethoven M, et al. CDK4/6 inhibition promotes antitumor immunity through the induction of T-cell memory. *Cancer Discov*. 2021;11(10):2582-2601.

37. Eisfeld AK, Kohlschmidt J, Schwind S, et al. Mutations in the CCND1 and CCND2 genes are frequent events in adult patients with t(8;21)(q22;q22) acute myeloid leukemia. *Leukemia*. 2017;31(6):1278-1285.

38. Wu SY, Yang J, Hong D, et al. Suppressed CCL2 expression inhibits the proliferation of leukemia cells via the cell cycle protein Cyclin D1: preliminary in vitro data. *Eur Rev Med Pharmacol Sci*. 2018;22(17):5588-5596.

39. Liu H, Wu H, Qin X. MicroRNA-206 serves as a tumor suppressor in pediatric acute myeloid leukemia by targeting Cyclin D1. *Pathol Res Pract*. 2019;215(10):152554.

40. Chen X, Burkhardt DB, Hartman AA, et al. MLL-AF9 initiates transformation from fast-proliferating myeloid progenitors. *Nat Commun*. 2019;10(1):5767.

41. Khaldoyanidi S, Nagorsen D, Stein A, Ossenkoppele G, Subklewe M. Immune biology of acute myeloid leukemia: implications for immunotherapy. *J Clin Oncol*. 2021;39(5):419-432.

42. Lamble AJ, Lind EF. Targeting the immune microenvironment in acute myeloid leukemia: a focus on T cell immunity. *Front Oncol*. 2018;8:213.

43. Binnewies M, Roberts EW, Kersten K, et al. Understanding the tumor immune microenvironment (TIME) for effective therapy. *Nat Med*. 2018;24(5):541-550.

44. Thorsson V, Gibbs DL, Brown SD, et al. The immune landscape of cancer. *Immunity*. 2018;48(4):812-830.e814.

45. Vadakekolathu J, Minden MD, Hood T, et al. Immune landscapes predict chemotherapy resistance and immunotherapy response in acute myeloid leukemia. *Sci Transl Med*. 2020;12(546):eaaz0463.

46. Benci JL, Xu B, Qiu Y, et al. Tumor interferon signaling regulates a multigenic resistance program to immune checkpoint blockade. *Cell*. 2016;167(6):1540-1554.e1512.

47. Cerezo M, Guemiri R, Druillennec S, et al. Translational control of tumor immune escape via the eIF4F-STAT1-PD-L1 axis in melanoma. *Nat Med*. 2018;24(12):1877-1886.

48. Abiko K, Matsumura N, Hamanishi J, et al. IFN-γ from lymphocytes induces PD-L1 expression and promotes progression of ovarian cancer. *Br J Cancer*. 2015;112(9):1501-1509.

49. Ayers M, Lunceford J, Nebozhyn M, et al. IFN-γ-related mRNA profile predicts clinical response to PD-1 blockade. *J Clin Invest*. 2017;127(8):2930-2940.

50. Vera Alvarez R, Pongor LS, Mariño-Ramírez L, Landsman D. TPMCalculator: one-step software to quantify mRNA abundance of genomic features. *Bioinformatics*. 2019;35(11):1960-1962.

51. Ley TJ, Miller C, Ding L, et al. Genomic and epigenomic landscapes of adult de novo acute myeloid leukemia. *N Engl J Med*. 2013;368(22):2059-2074.

52. Tyner JW, Tognon CE, Bottomly D, et al. Functional genomic landscape of acute myeloid leukaemia. *Nature*. 2018;562(7728):526-531.

53. Cerami E, Gao J, Dogrusoz U, et al. The cBio cancer genomics portal: an open platform for exploring multidimensional cancer genomics data. *Cancer Discov*. 2012;2(5):401-404.

54. Gao J, Aksoy BA, Dogrusoz U, et al. Integrative analysis of complex cancer genomics and clinical profiles using the cBioPortal. *Sci Signal*. 2013;6(269):pl1.

55. Newman AM, Steen CB, Liu CL, et al. Determining cell type abundance and expression from bulk tissues with digital cytometry. *Nat Biotechnol*. 2019;37(7):773-782.

56. van Galen P, Hovestadt V, Wadsworth Ii MH, et al. Single-cell RNA-seq reveals AML hierarchies relevant to disease progression and immunity. *Cell*. 2019;176(6):1265-1281.e1224.

57. Kataoka K, Sato T, Yoshimi A, et al. Evi1 is essential for hematopoietic stem cell self-renewal, and its expression marks hematopoietic cells with long-term multilineage repopulating activity. *J Exp Med*. 2011;208(12):2403-2416.

58. Arai S, Yoshimi A, Shimabe M, et al. Evi-1 is a transcriptional target of mixed-lineage leukemia oncoproteins in hematopoietic stem cells. *Blood*. 2011;117(23):6304-6314.

59. Wilson NK, Foster SD, Wang X, et al. Combinatorial transcriptional control in blood stem/progenitor cells: genome-wide analysis of ten major transcriptional regulators. *Cell Stem Cell*. 2010;7(4):532-544.

60. Castro-Mondragon JA, Riudavets-Puig R, Rauluseviciute I, et al. JASPAR 2022: the 9th release of the open-access database of transcription factor binding profiles. *Nucleic Acids Res*. 2021;50(D1):D165-D173.

61. Schütte J, Wang H, Antoniou S, et al. An experimentally validated network of nine haematopoietic transcription factors reveals mechanisms of cell state stability. *Elife*. 2016;5:e11469.

62. Kroon E, Krosl J, Thorsteinsdottir U, Baban S, Buchberg AM, Sauvageau G. Hoxa9 transforms primary bone marrow cells through specific collaboration with Meis1a but not Pbx1b. *EMBO J*. 1998;17(13):3714-3725.

63. Deguchi K, Ayton PM, Carapeti M, et al. MOZ-TIF2-induced acute myeloid leukemia requires the MOZ nucleosome binding motif and TIF2-mediated recruitment of CBP. *Cancer Cell*. 2003;3(3):259-271.

64. Mandoli A, Singh AA, Jansen PW, et al. CBFB-MYH11/RUNX1 together with a compendium of hematopoietic regulators, chromatin modifiers and basal transcription factors occupies self-renewal genes in inv(16) acute myeloid leukemia. *Leukemia*. 2014;28(4):770-778.

65. Mandoli A, Singh AA, Prange KHM, et al. The hematopoietic transcription factors RUNX1 and ERG prevent AML1-ETO oncogene overexpression and onset of the apoptosis program in t(8;21) AMLs. *Cell Rep*. 2016;17(8):2087-2100.

66. Oki S, Ohta T, Shioi G, et al. ChIP-Atlas: a data-mining suite powered by full integration of public ChIP-seq data. *EMBO Rep*. 2018;19(12):e46255.

67. Montalto FI, De Amicis F. Cyclin D1 in cancer: a molecular connection for cell cycle control, adhesion and invasion in tumor and stroma. *Cells*. 2020;9(12):2648.

68. Glass C, Wuertzer C, Cui X, et al. Global identification of EVI1 target genes in acute myeloid leukemia. *PLoS One*. 2013;8(6):e67134.

69. Zhang Y, Liu Z. STAT1 in cancer: friend or foe? *Discov Med*. 2017;24(130):19-29.

70. Kryczek I, Banerjee M, Cheng P, et al. Phenotype, distribution, generation, and functional and clinical relevance of Th17 cells in the human tumor environments. *Blood*. 2009;114(6):1141-1149.

71. Harlin H, Meng Y, Peterson AC, et al. Chemokine expression in melanoma metastases associated with CD8+ T-cell recruitment. *Cancer Res*. 2009;69(7):3077-3085.

72. Stavropoulou V, Kaspar S, Brault L, et al. MLL-AF9 expression in hematopoietic stem cells drives a highly invasive AML expressing EMT-related genes linked to poor outcome. *Cancer Cell*. 2016;30(1):43-58.

73. Krivtsov AV, Figueroa ME, Sinha AU, et al. Cell of origin determines clinically relevant subtypes of MLL-rearranged AML. *Leukemia*. 2013;27(4):852-860.

74. Schmöllerl J, Barbosa I, Minnich M. EVI1 drives leukemogenesis through aberrant ERG activation. *Blood*. 2023;141(5):453-466.

75. Xiong Y, Wang Y, Li T, et al. A novel function for cyclin D1 as a transcriptional role in oncogenesis and tumor development by ChIP-seq and RNA-seq. *J Cancer*. 2021;12(17):5181-5192.

76. Buonamici S, Li D, Mikhail FM, et al. EVI1 abrogates interferon-alpha response by selectively blocking PML induction. *J Biol Chem*. 2005;280(1):428-436.

77. Vadakekolathu J, Lai C, Reeder S, et al. TP53 abnormalities correlate with immune infiltration and associate with response to flotetuzumab immunotherapy in AML. *Blood Adv*. 2020;4(20):5011-5024.

78. You X, Liu F, Binder M, et al. Asxl1loss cooperates with oncogenic Nras in mice to reprogram immune microenvironment and drive leukemic transformation. *Blood*. 2022;139(7):1066-1079.